Kovove Mater. 54 2016 27–35
DOI: 10.4149/km_2016_1_27

Characterization of microstructure and strength of microwave welded Inconel 718 joints at 2.45 GHz frequency

A. Bansal[1], A. Kumar Sharma[1], S. Das[2], P. Kumar[1]

[1]*Department of Mechanical and Industrial Engineering, Indian Institute of Technology Roorkee, Roorkee-247667, India*
[2]*Reactor Control Division, BARC, Mumbai, India*

Received 4 June 2014, received in revised form 8 December 2014, accepted 9 February 2015

Abstract

Inconel 718 plates were butt welded through hybrid microwave heating (MHH) technique using Inconel 718 powder as a sandwich layer. Joining was affected through the fusion of the sandwich layer pre-placed between the bulk pieces owing to the heat generated while irradiated with 2.45 GHz microwaves for 480 s. Various phases present in the joint zone were detected using X-ray diffraction (XRD) while the microstructural features were characterized using an optical microscopy and scanning electron microscopy (SEM). The XRD patterns show the presence of Laves, $\delta(Ni_3Nb)$ and carbide phases in the joint zone along with the main matrix. The microstructural study also reveals that there is not any interfacial cracking and microfissure in the joint zone due to uniform heating associated with the MHH process. The average microhardness of the joint was observed to be 245 ± 20 HV. The average ultimate tensile strength of the joint was observed to be 780 MPa with 11.11 % elongation.

K e y w o r d s: microwave, Inconel 718, hybrid heating, microstructure, Laves phases

1. Introduction

Inconel 718 is a precipitation hardenable Ni and Fe-based superalloy widely used in high-temperature applications in aerospace, gas turbines, power and nuclear industries, pumps, and tooling due to its excellent corrosion and oxidation resistance at a temperature up to 650 ℃. The Ni-based superalloy was mainly strengthened by precipitation hardened cubic or spherical shaped Ni_3(Al, Ti) coherent precipitates having an ordered FCC L12 crystal structure prior to Inconel 718 [1]. The Ni_3(Al, Ti) coherent precipitates experienced a rapid precipitation of hardened phase when subjected to an intermediate temperature range. This rapid precipitation of hardened phase results in heat treatment associated cracking, which has been observed in the Ni-based superalloy such as Waspaloy, Rene 41, Inconel X750, and Udimet 700 [2]. On the other hand, Inconel 718 exhibits good weldability because of slow precipitation of the principle strengthening precipitate γ''-Ni_3Nb phase having a lens like a disc shaped body-centered tetragonal structure. This coherent precipitate provides more time for the alloy to obtain the required hardness and causes stress to be relieved or relaxed before hardening. This slow aging characteristic of Inconel 718 enhances its resistance to cracking during post weld heat treatment. However, the addition of Nb in the alloy significantly reduces the strain age cracking problem, but it arises another problem of liquation cracking (microfissuring) in HAZ [3, 4]. The microfissures usually occur perpendicular to fusion boundary or under the tail head. The combination of grain boundary liquation and tensile stresses results in microfissure in the heat affected zone (HAZ) of Inconel 718 weld [5]. Another main problem for Inconel 718 alloy is the segregation of element Nb and consequently the formation of Nb-rich Laves phases, a brittle intermetallic compound found inside the weld and at the boundary in the HAZ. It can be denoted by a nominal formula of MN_2. Here Nb, Mo, and Ti are assigned to represent the larger M atom and Ni, Fe, and Cr the N-type atom [6]. It has been reported that formation of Laves phases is detrimental to weld mechanical properties because (i) it depletes the main matrix from the principal strengthening elements by

*Corresponding author: tel.: 8439869002; fax: 91-1332-285421; e-mail address: amit.bansal978@gmail.com

consuming significant amount of these strengthening elements, (ii) it forms a weak zone microstructure between the Laves phase and matrix interface, (iii) it acts as a nucleating site for crack initiation and propagation because of its inherent brittle nature, and deteriorates the mechanical properties of weld metal like tensile ductility, fracture toughness, fatigue and creep rupture properties [7–10]. As the presence of Laves phases in Inconel 718 weld is detrimental, efforts should be made to minimize the formation of Laves phases by reducing the segregation during weld metal solidification. The comparison of Nb segregation and formation of Laves phases in gas tungsten arc (GTA) and electron beam (EB) welding of Inconel 718 has been reported by Radhakrishna and Rao [11, 12]. The authors have discussed the advantages of using lower heat input processes for welding alloy to reduce the Laves phases in the weld metal. Murthy [13] discussed the advantages of oscillation beam technique for controlling Nb segregation and Laves formation in alloy 718 EB weld. Ram et al. [9] illustrated the advantage of using pulsed laser welding for controlling Nb segregation and consequently the formation of Laves phases at different post-weld heat treatment.

In all welding processes discussed above, the transfer of heat takes place through the conventional mode of heat transfer. Hence, there exists a thermal gradient that causes microfissures in the Inconel 718 weld. On the other hand, in microwave processing of materials, there is energy conversion rather than energy transfer, which dominates conventional processing of materials [14, 15]. Microwave heating is gaining popularity due to its specific advantages such as reduced processing time, low power consumption, enhanced product quality due to volumetric heating and less environmental hazards [16].

Processing of metal-based materials using microwave energy is challenging owing to reflection of microwaves by bulk metallic materials at room temperature due to their low skin depth. The successful joining of bulk metallic materials using MHH was first reported by Sharma et al. in the form of a patent [17]. Srinath et al. [18, 19] reported joining of similar as well as dissimilar materials using MHH. This paper discusses the joining of superalloy Inconel 718 plates using the hybrid microwave heating (MHH) technique in a multimode microwave applicator, and characterization of the joints in respect of microstructure, microhardness, and tensile strength.

2. Experimental details

In the present work, butt joining of Inconel 718 plates has been accomplished using Inconel 718 powder as an interface layer. The experimental procedure adopted is briefly described in the following sections.

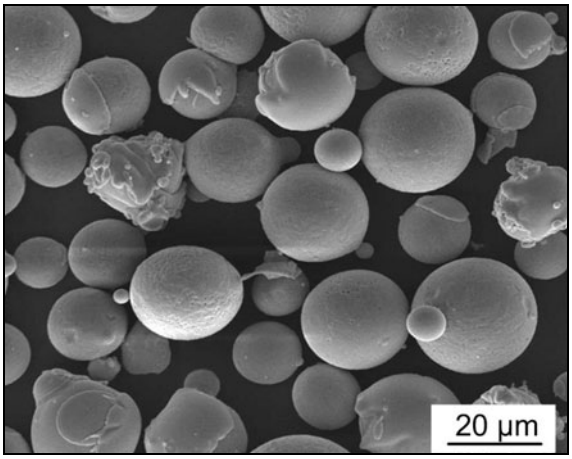

Fig. 1. SEM micrograph of the Inconel 718 powder.

2.1. Material selection

Inconel 718 plates having dimensions of 25 × 10 × 4 mm^3 in solution treated condition (980 ℃ for 1 h and then air cooled) were used as the base material. Joints were made in the form of butt configuration. The slurry of Inconel 718 powder was prepared by mixing it with an epoxy resin (Bisphenol-A, Blumer 1450XX). The prepared slurry was filled between the interfacing surfaces to be joined with an approximate thickness of 0.5 mm. The SEM micrograph (Fig. 1) shows the typical spherical morphology of the Inconel 718 powder used as an interface layer. The chemical composition of Inconel 718 powder and Inconel 718 plates provided by the supplier are given in Table 1.

2.2. Development of joints

The Inconel 718 plates were placed in butt joining configuration on alumina plate, and the prepared slurry was filled manually between the interfacing surfaces to be joined (a gap thickness approximately 0.5 mm). The alumina plate acts as a separator between the insulating material and the fusion zone. The experiments were performed in an insulating box (Make: Enerzi Microwave Systems Pvt. Ltd.), which is exposed to microwave radiation in a domestic microwave oven for 480 s at 2.45 GHz and 900 W. There exists an optimal time of exposure at 900 W and for proper fusion of the interfacing surfaces with the interfacing powder particles. The optimum time has been observed to be 480 s in the present study. The refractory box is transparent to microwaves due to low dielectric loss, and it also acts as a thermal insulator. Various processing parameters used in this experiment are summarized in Table 2.

Table 1. Elemental composition of materials used

Material	Elements composition (wt.%)											
	Fe	Cr	Ni	Mo	P	Si	S	C	Nb	Ti	Al	B
Inconel 718 plates	Bal.	17.7	52.6	3.13	0.005	0.03	0.002	0.02	5.08	0.97	0.51	0.003
Inconel 718 powder	Bal.	17.7	53.5	2.92	0.005	0.03	0.002	0.02	5.215	0.97	0.55	0.003

Table 2. Microwave processing parameters used for joining Inconel 718 plates

Parameters	Description
Applicator	Multimode (Make: LG, Model: Solar Dom)
Base material	Inconel 718 plates
Frequency	2.45 GHz
Interfacing powder layer	Inconel 718 powder in slurry form
Susceptor material	SiC plate 25 × 10 × 6 mm^3
Flux material	UV 420 TT
Exposure power	900 W
Exposure time	480 s

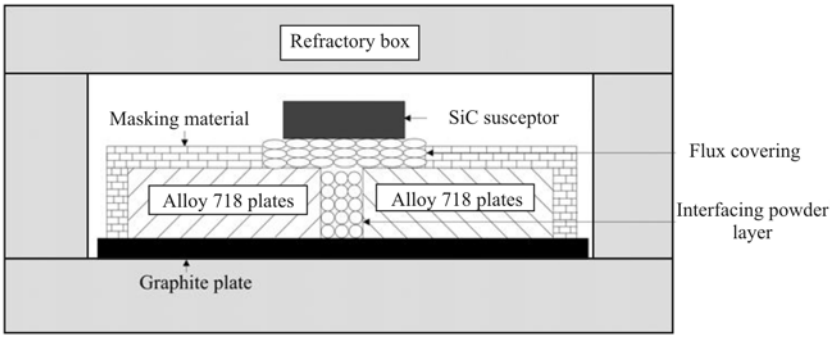

Fig. 2. Schematic diagram of the MHH process used for making a joint.

Bulk alloy 718 reflects microwave radiation at 2.45 GHz due to the low skin depth. Hence, the bulk pieces were masked with an insulator to prevent its direct coupling with microwaves. The skin depth of nickel, the main constituent of Inconel 718 powder was calculated to be 0.12 μm [20], which is less than the size of the interface powder particles. Hence, the powder particles do not absorb microwaves at room temperature. Thus, for effective coupling of the powder particles, the principles of MHH were applied. In MHH, suspectors that are good absorbers of microwaves at room temperature were used for providing initial heating to a target material using conventional mode of heat transfer. Consequently, at high temperature, the material itself starts absorbing microwaves due to increasing skin depth. In this experiment, SiC was used as a suspector for providing initial heating to powder particles, and consequently at elevated temperature the powder particles start absorbing microwave radiation. Figure 2 illustrates the schematic view of the experimental setup used for joining of Inconel 718 plates using MHH. To avoid the interaction of fusion zone with air at high temperature, the flux UV 420 TT was used. The flux used was preheated in a muffle furnace at 250℃ to remove any possibility of moisture. The flux melted at high temperature and formed a slag in the fusion zone. It provides protection to the weld pool from atmospheric gases. Slag is lighter than the weld pool, and it has a lower melting point than the weld pool. Hence, as the weld pool gets solidified, the slag forms on the surface of the molten pool. This slag retards the cooling rate, thus helps in controlling the defects like cracking or porosity formation because gases dissolved in the weld pool have enough time to come from the weld pool during solidification.

The joint specimens were taken from the insulating material, and the slag was removed manually. On cooling, the molten sandwich layer becomes the 'weld bead' of the fusion joint. An optical micrograph of

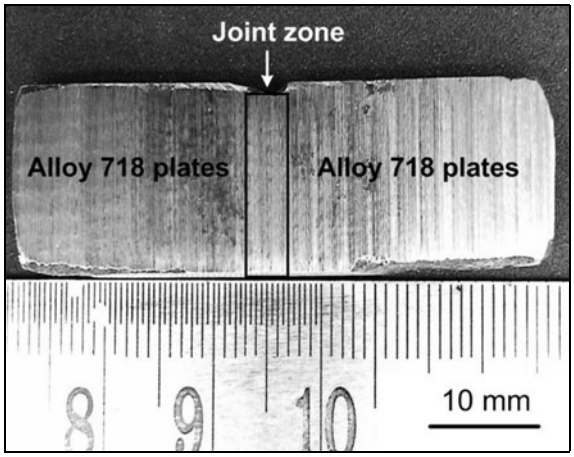

Fig. 3. An optical micrograph of the welded specimen.

the typical joint developed through MHH is shown in Fig. 3.

2.3. Characterization of the joints

Specimens for microstructural characterization were prepared according to standard metallographic methods. The polished samples were etched with Keller's reagent (100 ml methanol, 5 g cupric chloride, and 100 ml hydrochloric acid). Different phases formed in the joint zone were identified using XRD spectra taken at room temperature with Cu Kα radiation. The scan rate was maintained at 0.5 min^{-1} and scan range was used from 10° to 90°. Microstructural features of the joints were analyzed using the optical and field emission scanning electron microscope (FE-SEM) equipped with an energy dispersive X-ray detector (Make: EFI, Model: Quanta 200 FEG). The micro-indentation hardness measurements were taken across the joint zone at a load of 25 g for 10 s. The tensile tests were performed on a microwave welded joint using a universal testing machine (Make: INSTRON, Model: 5982) at a uniform strain rate of 0.2 mm s^{-1}. The specimens were prepared according to ASTM standard with 18 mm gauge length and 3.5 mm width. Five samples were tested, and the average values have been reported. The fractured samples were subsequently studied for fractographic observations using a scanning electron microscope.

3. Results and discussion

In the present work, metallurgical bonding of Inconel 718 plates has been accomplished through complete melting of the interface powder layer of the same material. Typical characterization results

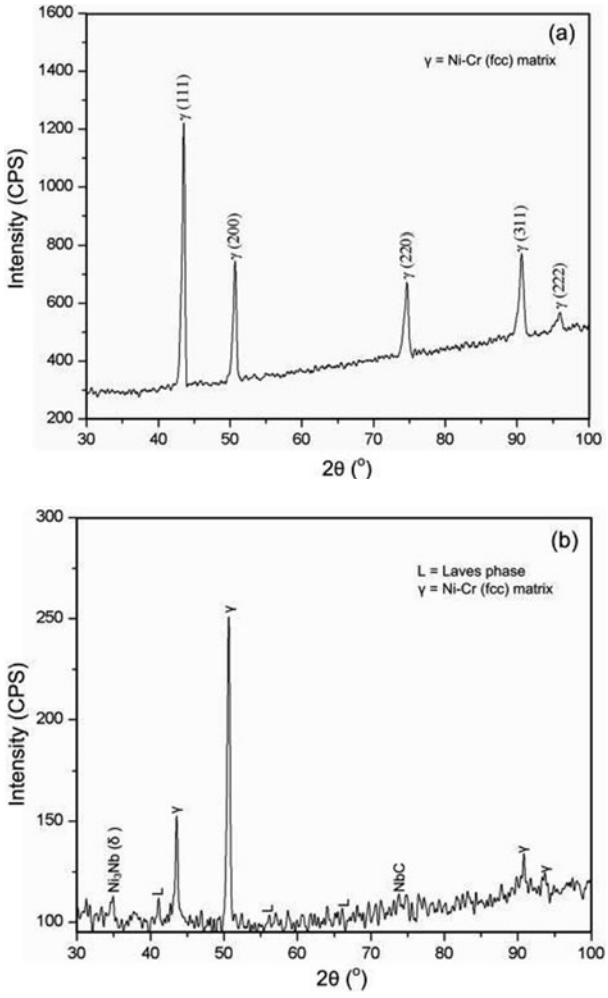

Fig. 4. Typical XRD spectra of (a) initial Inconel 718 powder, and (b) the joint zone developed through MHH technique.

of the developed joints are discussed with suitable illustrations in the following sections.

3.1. X-ray diffraction results

The typical XRD spectrum of starting Inconel 718 powder shows the dominant presence of γ (111) phases, where γ is a Ni-Cr (a = 0.359 nm, space group Fm-3m) rich solid solution with face-centered cubic (fcc) structure (Fig. 4a). On the other hand, the XRD spectrum of the joint zone (Fig. 4b) shows the presence of Laves, Ni_3Nb type δ and niobium carbide (NbC) phases along with the fcc matrix. Further, the major peak corresponding to γ (111) with a 2θ value of 43.5° has significantly attenuated (Fig. 4b). In the interfacing powder layer, the alloying elements, which were present in the form of a solid solution, react with each other and other elements, got diffused from the interfacing surfaces during MHH; consequently formation of a new phase takes place. The formation

Table 3. Relative phase intensity of dissimilar metal welding

S. No.	Phase	I_1	I_2	I_3	I_4	I_{back}	NIR (%)
1	δ-Ni_3Nb	113				100	6.83
2	Laves		113.5			100	6.98
3	Matrix			250		100	78.82
4	NbC				114	100	7.35

of these new phases is attributed to rapid heating of Inconel 718 powder during microwave exposure and sudden removal of heat source associated with the end of irradiation cycle. However, the flux used in this process prevents the interaction of fusion zone with the atmosphere at high temperature. It significantly reduces the cooling rate after the end of irradiation cycle. In slow cooling rate, the elements have enough time to react with each other at high temperature and consequently the formation of new phases, mainly Laves phases occurred. These new phases have a significant effect on the joint properties because they consume an alloying element required for strengthening the matrix. For formation of Laves phase at least 10 to 12 % Nb is required. The formation of Laves phase in the interdendritic region is explained with the help of following reactions:

$$\text{Liquid} \rightarrow \text{Liquid enriched with Nb} + \gamma, \quad (1)$$

$$\text{Liquid enriched with Nb} \rightarrow \gamma + \text{Laves}. \quad (2)$$

The second reaction corresponds to the eutectic reaction, and it terminates the solidification process. The formation of NbC is attributed to the fact that the equilibrium distribution coefficient of Nb is less than 1; therefore it easily got distributed into the interdendritic regions during solidification and consequently a formation of Nb-enriched carbides takes place. The different phases present in the joint zone were further determined using relative peak intensity ratio of the respective phases. The peak intensity value of different phases detected in the XRD spectrum (Fig. 4b) is illustrated in Table 3. The normalized intensity ratio (NIR) of phase (1) was determined using the following Eq. (1) [21]:

$$\text{NIR}_1 = \frac{I_1 - I_{\text{back}}}{I_1 + I_2 + I_3 + I_4 - 4I_{\text{back}}}, \quad (3)$$

where I_1, I_2, I_3, and I_4 designate the intensities of 1^{st}, 2^{nd}, 3^{rd}, and 4^{th} phases, respectively, and I_{back} denotes the background intensity. The same relation, Eq. (3), was used for determining the NIR value for other phases. The major peak corresponding to that phase was considered in the XRD spectrum for calculating the NIR of different phases. However, the NIR value may not provide the accurate amount of phases present in the joint zone; yet, it provides a relative representation of the amount of phases present in the joint zone. Thus, from Table 3, it is observed that during microwave exposure, approximately 21.18 % of Inconel powder was transformed to niobium carbide, Laves phase and other intermetallic (δ Ni_3Nb) phases.

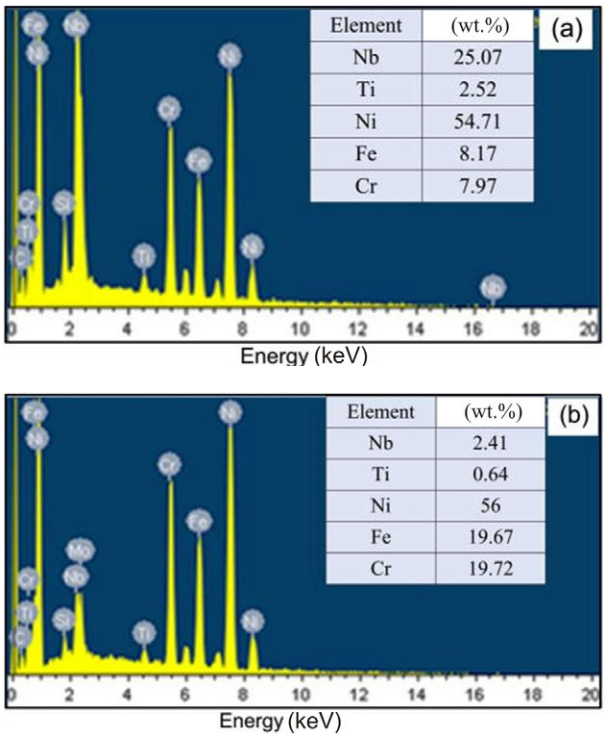

Fig. 5. Typical EDS spectra of the fusion zone (a) on Laves phases, and (b) inside the matrix.

3.2. Elemental study

Elemental composition of the welded joints was ascertained by an energy dispersive X-ray (EDX) microanalysis. As the fusion zone mainly consists of two parts – the matrix and the Laves phase, the composition points were taken inside the matrix and on the Laves phase. The corresponding EDS spectra are shown in Fig. 5. The major elements present in weight percentage are also shown in Fig. 5. It has been found that the interdendritic region (Laves phase) becomes enriched in Nb, Mo, Ti, and Si

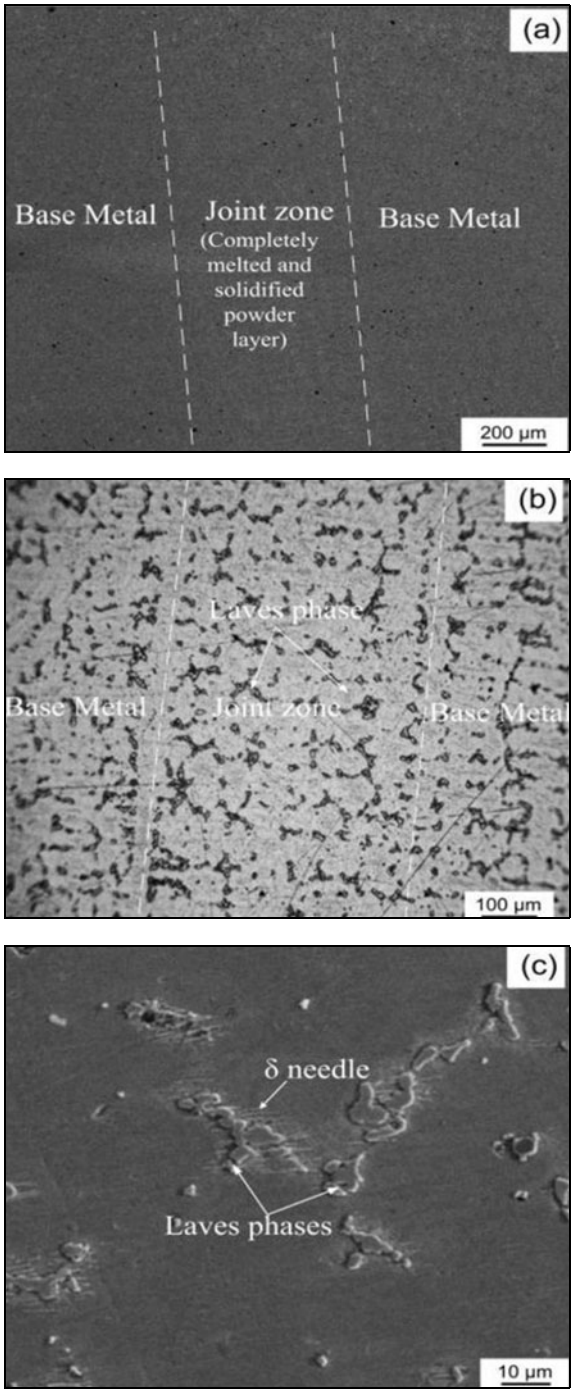

Fig. 6. The microstructure of the joint zone (a) back-scattered electron (BSE) micrograph, (b) optical micrograph, (c) SEM micrograph (1000 ×) of the fusion zone shows the presence of δ needle along with Laves phase.

while the dendritic core region was depleted of these strengthening elements. The dendritic core region has higher concentrations of Ni, Cr, and Fe compared to base metal composition, which is consistent with the findings of earlier investigations using electron probe micro analyzer [12].

3.3. SEM observation

A typical back-scattered electron (BSE) of the joint developed by MHH is shown in Fig. 6a. In the fusion zone, the interdendritic regions consisting of Laves phases and other hard particles got etched more and appear darker than the core as shown in optical micrograph (Fig. 6b). Inconel 718 is an alloying material, which solidified in a dendritic mode. The Laves phases appear to be distributed uniformly in the fusion zone due to a uniform temperature associated with MHH process. However, in the case of laser welding, the centre of fusion zone has finer and discrete phase and the fusion zone boundary has coarser and interconnected Laves phases due to the relatively high cooling rate observed at the centre of fusion zone as compared to fusion boundary [9]. The slightly coarser Laves phases form in the fusion zone as shown in Fig. 6b. However, in the case of laser welding due to rapid cooling rate inherent with laser welding process the solubility is limited, which reduces the segregation of alloying element. Hence, fine and discrete Laves phases are formed in the fusion zone. The formation of coarser Laves phases is due to a flux that was used for preventing the fusion zone to react with the atmosphere at high temperature. However, the flux reduces the cooling rate, so the porosity and intergranular cracking in the fusion zone and HAZ are reduced, which is inevitable in laser welding due to the fast cooling rate associated with laser welding process. However, due to slow cooling rate experienced by fusion zone, the useful alloying elements like Nb, Mo, and Ti, which are required for the formation of strengthening phases, diffuse and segregate in the interdendritic region, and formation of Nb-rich Laves phase takes place. Thus, cooling rate and heat input of welding process significantly influence the segregation of useful strengthening elements. Solidification of Inconel 718 starts with a primary Liquid $\rightarrow \gamma$ reaction and proceeds, causing an enrichment of interdendritic liquid in Nb, Mo, Ti, Si, and C, until a eutectic type reaction Liquid $\rightarrow$ (γ + Laves) occurs, terminating the solidification process [22]. Thus, the formation of Laves phases is due to interdendritic Nb segregation. The Laves phases are detrimental to weld mechanical properties because they are hard and brittle in nature. Any crack that initiates to propagate inside the Laves phase thus reduces the weld fatigue and other mechanical properties. The crack grew predominantly through Laves phases only. Although the joint contains the NbC and Laves phases, there is not any evidence of microfissure in the joint zone or HAZ. This is attributed to the absence of rapid thermal cycle of HAZ and joint zone, which usually occurs in laser welding due to high cooling rate. The uniform heating associated with MHH process results in the absence

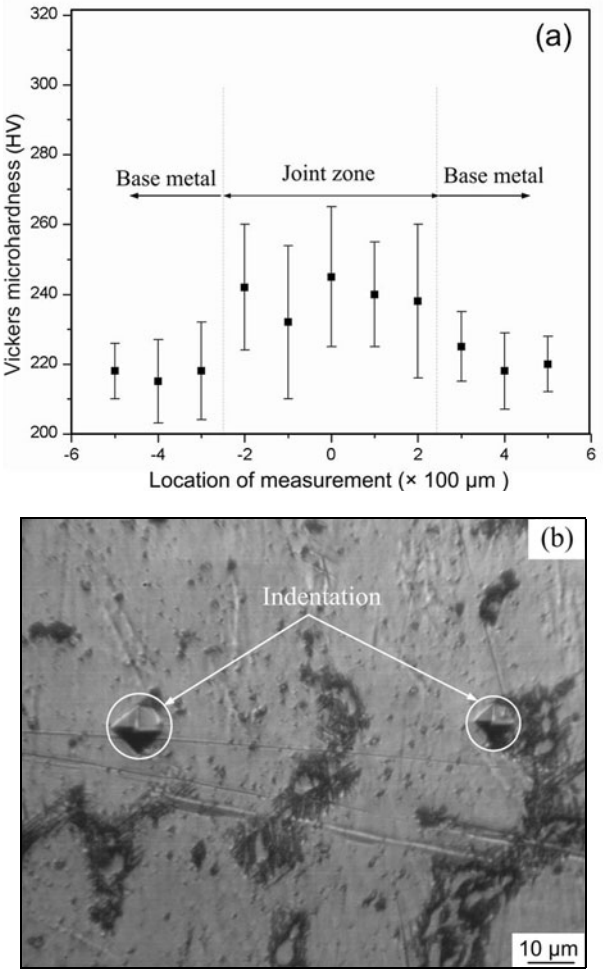

Fig. 7. (a) Microhardness profile across the weld zone and (b) typical morphology of the indentation made in the Laves phase and the matrix.

of microfissures in the joint zone and HAZ. Another important observation is the formation of δ phase having a needle-like structure along with Laves phases as shown in SEM secondary image of the fusion zone taken at higher magnification (Fig. 6c). The Laves phases appear brighter (Fig. 6c) in the fusion zone of joint due to the higher emission of electrons from these phases [23]. The δ phase is an orthorhombic precipitate, and it precipitates in the range of 860 to 995 ℃. The δ phase forms near the Laves phase having higher Nb concentration. The presence of Laves phase favours the formation of δ phase by providing sites for the nucleation of δ phase. This is the reason the δ phase precipitation takes place exclusively around Laves particle.

It is clearly seen in Fig. 6b that the interface is free from any visible cracking, and it has good metallurgical bonding with the substrate. A continuous weld line without any mixed zone is observed along the interface. The formation of the unmixed

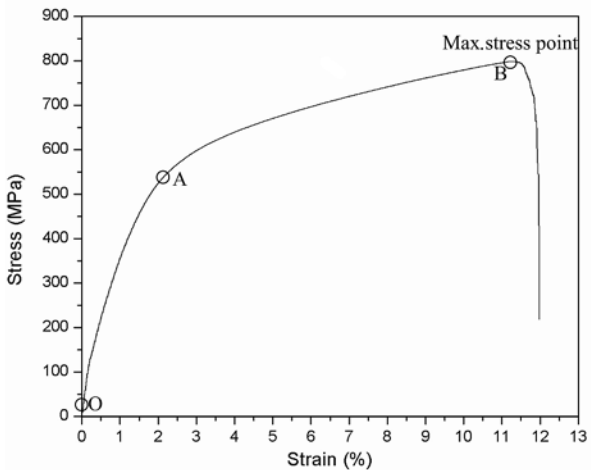

Fig. 8. A typical stress-strain curve for the tested welded specimen.

zone is attributed to the fact that both base metal and powder particle to be used are of the same composition. The HAZ produced is very low due to localized melting of predominantly powder particles during microwave exposures.

3.4. Microhardness study

The microhardness of the welded joint was evaluated across the joint. The distance between two successive indentations was kept at 100 μm. Three indentations were made laterally at each location, and the mean was considered. Figure 7a illustrates the distribution of the microhardness values. The measured microhardness has different values at different phases, which is attributed to varying microhardness of different phases. The microhardness value is higher for Laves phases (550 HV) than the base metal matrix (220 HV). The morphology of typical indentation made on the Laves phases and inside the matrix is shown in Fig. 7b. The indentations have different morphology made on Laves phase and inside the matrix, which is characterizing a difference in the inherent properties of Laves phase and the matrix. The average microhardness observed in the fusion zone and base metal was 240 $\pm$ 20 HV and 220 $\pm$ 10 HV, respectively. The low microhardness observed at the fusion zone as compared to laser welding was due to the slow cooling rate observed at the fusion zone due to the presence of the flux covering. Also, the coarser Laves phases are incoherent in nature, and they contribute very little to increasing the hardness of the main matrix.

3.5. Observation on tensile strength and fractography study

The joints were subjected to tensile loading as

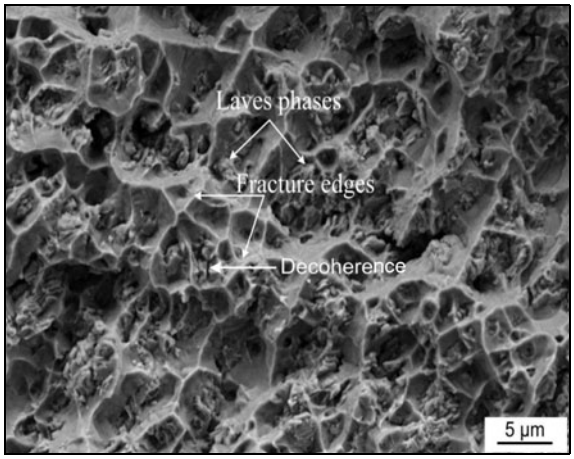

Fig. 9. SEM micrograph of the fracture surface.

per ASTM testing procedure. A typical tensile test characteristics obtained during the test is presented in Fig. 8. From Fig. 8, it has been found that the curve 'OA' represents the elastic deformation of the welded specimen, i.e. stress is proportional to strain in this part of the curve, and after point 'A' plastic deformation in the material begins. Point 'B' indicates the maximum stress sustained by the welded specimen during tensile loading. An average ultimate strength of 780 MPa with an elongation of 11.11 % was recorded. The fractured surfaces of the failure specimens were further analyzed by SEM to understand structure-property-fracture correlations. A typical SEM micrograph of the fractured surface is shown in Fig. 9, which shows the dimpled rupture with the presence of Laves phases inside the dimples. As the tensile load is applied, matrix deforms plastically by the mechanism of slip. However, the Laves phases present in the matrix do not deform plastically along with the matrix as they are hard and brittle in nature. Moreover, the Laves phases are incoherent in nature with high interfacial energy. For plastic deformation to take place in the material, movement of dislocation in the material is necessary, because Laves phases are incoherent. Hence, there is not any continuity of lattice planes across the interface between the matrix and the Laves phases. Hence, the dislocations are moving inside the matrix by passing these incoherent precipitates (Laves phases). In this way, the microvoids are initiated along with the matrix and Laves phases. Further, there is an occasional spalling of the Laves phases as they decohere from the basic matrix structure. Thus, the Laves phases present in the matrix make the initiation of fracture process by rendering favourable sites for microvoid initiation and consequently the growth of macroscopic cracks along Laves/matrix interface.

4. Conclusions

A novel method for butt joining of Inconel 718 plates through MHH technique using Inconel 718 powder as an interfacing layer has been demonstrated. The mechanism of the joint formation has been explained. Major conclusions drawn from the present work include the following:

1. Fusion joining of Inconel 718 plates is possible using microwave energy at 900 W and 2.45 GHz.
2. Inconel 718 plates are metallurgically bonded through Inconel 718 powder interfacing layer by partial mutual diffusion of elements and complete melting of powder particles.
3. The joints are free from any interfacial cracks and microfissures in the joint zone and HAZ, which can be attributed to a uniform heating associated with MHH process with a minimal thermal gradient.
4. The formation of Laves, δ and carbide phases takes place along with the matrix during microwave exposures.
5. The average microhardness is observed to be within a narrow band of 240 HV($\pm$ 20) on a fusion zone and base metal while the microhardness of the Laves phase is approximately double than the joint base matrix hardness. The close scatter of the microhardness of the joints is attributed to volumetric heating during the MHH process.
6. The average ultimate tensile strength of the joints was observed to be about 86 % of the base material strength (about 900 MPa). However, a significant elongation of the joints about 11.11 % could be monitored. The Laves phases present in the matrix initiate the fracture process by providing favourable sites for microvoid initiation and growth of macroscopic cracks along Laves/matrix interfaces.

Acknowledgements

The authors would like to express gratefulness to the Board of Research in Nuclear Sciences (BRNS), Department of Atomic Energy, Government of India, for financing this work with project No. 2010/36/60-BRNS/2048.

References

[1] Lingenfelter, A.: In: Proceedings of Conference "Superalloy 718 – Metallurgy and Applications". Ed.: Loria, E. A. Warrendale, TMS-AIME 1989, p. 673.
[2] Ping, D. H., Gu, Y. E., Cui, C. Y., Harada, H.: Mater. Sci. Eng. A, *456*, 2007, p. 99. doi:10.1016/j.msea.2007.01.090
[3] Tillack, D. J.: Weld. J., *1*, 2007, p. 28.
[4] Gobbi, S., Zhang, L., Norris, J., Richter, K. H., Loreau, J. H.: J. Mater. Process. Technol., *56*, 1996, p. 333. doi:10.1016/0924-0136(95)01847-6

[5] Thompson, R. G.: J. Metals, *40*, 1988, p. 44. doi:10.1007/BF03258151
[6] Vincent, R.: Acta Metall., *33*, 1985, p. 1205. doi:10.1016/0001-6160(85)90231-7
[7] Fontana, G., Gobbi, S., Rivela, C., Zhang, L.: Weld Int., *13*, 1999, p. 631. doi:10.1080/09507119909447423
[8] Cornu, D., Gouhier, D., Richard, I., Bobin, V., Boudot, C., Gaudin, J. P., Andrzejewski, H., Grevey, D., Portrat, J.: Weld Int., *9*, 1995, p. 802. doi:10.1080/09507119509548898
[9] Ram, G. D. J., Reddy, A. V., Rao, K. P., Reddy, G. M., Sundar, J. K. S.: J. Mater. Process. Technol., *167*, 2005, p. 73. doi:10.1016/j.jmatprotec.2004.09.081
[10] Biswas, S., Reddy, G. M., Mohandas, T., Murthy, C. V. S.: J. Mater. Sci., *39*, 2004, p. 6813. doi:10.1023/B:JMSC.0000045609.86430.19
[11] Radhakrishna, C. H., Rao, K. P.: Mater. High Temp., *12*, 1994, p. 323.
[12] Radhakrishna, C. H., Rao, K. P.: J. Mater. Sci., *32*, 1997, p. 1977. doi:10.1023/A:1018541915113
[13] Murthy, C. V. S.: Electron Beam Welding of Alloy 718 – a Study on the Effects of Beam Oscillation Technique. [M. Sc. Thesis]. Madras, Indian Institute of Technology 2004.
[14] Clark, D. E., Folz, C. E., West, J. K.: Mater. Sci. Eng. A, *287*, 2000, p. 153. doi:10.1016/S0921-5093(00)00768-1
[15] Clark, D. E., Sutton, W. H.: Annu. Rev. Mater. Sci., *26*, 1996, p. 299. doi:10.1146/annurev.ms.26.080196.001503
[16] Ku, H. S., Siores, E., Taube, A., Ball, J. A. R.: Comput. Ind. Eng., *42*, 2002, p. 281. doi:10.1016/S0360-8352(02)00026-8
[17] Sharma, A. K., Srinath, M. S., Kumar, P.: A Method of Joining of Bulk Metallic Materials by Microwave Hybrid Heating. Indian Patent Application No. 1994/DEL/2009.
[18] Srinath, M. S., Sharma, A. K., Kumar, P.: Mater. Des., *32*, 2011, p. 2685. doi:10.1016/j.matdes.2011.01.023
[19] Srinath, M. S., Sharma, A. K., Kumar, P.: Journal of Manufacturing Processes, *13*, 2011, p. 141. doi:10.1016/j.jmapro.2011.03.001
[20] Gupta, D., Sharma, A. K.: Surf. Coat. Technol., *205*, 2011, p. 5147. doi:10.1016/j.surfcoat.2011.05.018
[21] Peelamedu, R., Agrawal, D., Roy, R.: Mater. Lett., *55*, 2002, p. 234. doi:10.1016/S0167-577X(01)00653-X
[22] Sivaprasad, K., Raman, S. G. S.: Metall. Mater. Trans. A, *39A*, 2008, p. 2115. doi:10.1007/s11661-008-9553-y
[23] Dupont, J. N., Robino, C. V., Marder, A. R.: Weld. J., *77*, 1998, p. 417.